Research Article

Journal of Environmental Nanotechnology

Impact of Fiber Orientation on the Mechanical Characteristics of Hybrid Banana Palm Amino Composites and AI-based Performance Prediction

Dipti N. Kashyap[1], Shrikant R. Jachak[1], Sandip S. Khedkar[1], Maheskumar Ponnuswamy[2], G. Suresh[3], R. Revathi[4] and S. Mayakannan[5,6]*

[1]Department of Mechanical Engineering, Yeshwantrao Chavan College of Engineering, Wanadongri, Nagpur, MH, India
[2]Department of Mechanical Engineering, Nandha College of Technology, Perundurai, Erode, TN, India
[3]Department of Mathematics, Vel Tech High Tech Dr.Rangarajan Dr.Sakunthala Engineering College, Avadi, Chennai, TN, India
[4]Department of Electronics and Communication Engineering, Koneru Lakshmaiah Education foundation, Vaddeswaram, Guntur, AP, India
[5]Department of Mechanical Engineering, Rathinam Technical Campus, Coimbatore, TN, India
[6]Department of Mechanical Engineering, Saveetha School of Engineering, Saveetha Institute of Medical and Technical Sciences, Chennai, TN, India
Received: 25.07.2025 Accepted: 18.09.2025 Published: 30.09.2025
*kannanarchieves@gmail.com

ABSTRACT

This research utilized the compression technique to produce hybrid composite layers of equal amounts of Palm fiber and Banana fiber with varying fiber alignments [0/0/0/0/0/0(S1), 0/45/0/0/45/0(S2), 0/90/0/0/90/0 (S3), and +45/−45/+45/+45/−45/+45 (S4)], incorporated in amino resin matrix with TiO_2 as a nanofiller. The effect of fiber direction on natural fiber composites was assessed by tensile strength (TS), flexural strength (FS), impact strength (IS), and interlaminar shear strength tests (ILSS), performed. Furthermore, a comprehensive statistical analysis was conducted using Machine Learning methods such as artificial neural networks (ANN) for predictive purposes. Composite density is greatly affected by voids and imperfections, as shown by the experimental results, in the intervals (0/45/0/0/45/0). The experimental density and void content of composite S2 were higher than those of the other composites. In comparison to other composites, composite S1 (0/0/0/0/0/0) had a 5% to 29% higher flexural load-bearing capacity, impact strength, and tensile strength. Composite S1, a fiber-oriented composite, demonstrated the highest interlaminar shear strength value of 3.35 MPa compared to other composites. Scanning electron microscope (SEM) analysis revealed a beneficial interaction between amino resin and Banana-Palm eco fibers within the composite. It accurately estimates strengths with high R^2 ratings of 1, 0.98, and 0.99 for TS, FS, and IS. The interaction coefficients of the model are approximately 1, indicating strong correlative and predictive significance.

Keywords: Flexural strength; Composite materials; Natural fibers; Artificial neural networks; Mechanical properties.

1. INTRODUCTION

Growing public concern over environmental issues, high environmental regulations, and the unsustainable use of petroleum resources have collectively driven the development of eco-friendly products. Natural fibers are considered more environmentally friendly materials than synthetic fibers due to their superior characteristics. Fiber composites with NaOH-treated fibers showed flexural strength and fracture toughness, while reducing moisture absorption (Venkatesh, 2024). A bioresin was developed and used to fabricate composites with fibers and particles (Kandavalli *et al.* 2025). Singh *et al.* (2024) reported that chitosan-treated fibers could be successfully employed to reinforce polypropylene composites through film-stacking compression molding. Tensile properties were evaluated by Girimurugan *et al.* (2022) for three composite variants as per ASTM standards. Nano-alumina addition significantly improved tensile behavior of the fabricated composites. The best combination yielded 24.75 MPa tensile, 31.25 MPa flexural, and 21.47 kJ/m^2 impact strength, with potential for environmental applications (Gowrishankar *et al.* 2025). Flexural strength and hardness showed strong correlation between predicted and experimental values ($R^2 > 0.95$). Design-Expert modeling confirmed accuracy and reliability of the optimized composite configuration (Arunachalam and Saravanan, 2024). Epoxy composites with optimized ply-stacking sequences demonstrated enhanced mechanical properties, especially in tensile and flexural strength, as observed by Muralidharan *et al.* (2022).

Natural hybrid composites using natural fiber and nanopowder achieved high mechanical and thermal properties (Kumar *et al.* 2024). Four laminates of polyester mats and sheaths were hot-pressed with different stacking sequences to study mechanical and

acoustic properties. The polyester fiber mats (WFs) and palm sheaths (WPs) of WP/WP/WF/WP/WF laminate showed flexural and tensile strength improvements over pure composites (Tang *et al.* 2024). Hybrid polymer nanocomposites were fabricated using banana fibers, epoxy, and nanopowder with ultrasonication for uniform dispersion. Mechanical testing showed peak values at 0.50 wt.% tensile, 525.56 MPa, flexural, and 52.23 MPa ILSS (Shubham *et al.* 2024). Natural and synthetic fiber-reinforced epoxy composites were fabricated in three stacking sequences using vacuum-assisted compression molding. Type III composite (aloe vera + palmyra palm + synthetic fiber) showed a 12–30% increase in tensile strength and 11–13% in flexural strength over other types. Better wettability between aloe vera/palmyra palm and matrix contributed to enhanced performance (Banu *et al.* 2021). Water absorption behavior of bio-composites reinforced with fibers was analyzed across seawater, distilled water, and rainwater for over 670 hours. Water uptake increased with fiber content due to high porosity (above 51%), with absorption ranging from ~14% to 42%. ANN prediction models achieved high accuracy ($R^2 > 0.99$) and minimal error (3×10^{-5}) (Benyettou *et al.* 2022). Natural fibers and nanosheets were used to create nano-hybrid polypropylene composites. Fiber content supported high tensile strength (45.4 MPa), flexural strength (62 MPa), and impact strength (147 J/m). FESEM showed improved fiber-matrix bonding and crack resistance for automotive/aerospace applications (Krishnasamy *et al.* 2025). The combination of optimized stacking sequence and nanoparticle reinforcement resulted in the highest ILSS, as reported by Giridharan and Sivaganesan, (2025).

Hybrid flax (F) /bamboo (B) epoxy composites were developed with four different stacking sequences to analyze mechanical and water absorption properties. The B/F/F/B configuration showed optimal performance with up to 25% flexural and 14.6% ILSS improvement (Vijayakumar *et al.* 2022). A sandwich-structured impact-resistant glass was developed using silicate glass skins and oil palm fiber–epoxy interlayers. Compressive strength improved from 280.60 MPa to 402.46 MPa with oil palm fiber addition, which also improved crack resistance. SEM revealed rough fibril morphology, aiding stress distribution and structural durability for construction use (Yuhari and Awang, 2023). ANN models predicted Young's modulus, stress, and strain with good accuracy ($R^2 = 0.87$) (Makri *et al.* 2024). FESEM showed microfibrils and rough surfaces suitable for bonding. The thermal stability and structural morphology of the filler support its use in polymeric composites for high-strength applications (Balan *et al.* 2025). Natrayan *et al.* (2023) optimized mechanical properties of fiber/nanofiller hybrid composites using ANN methods. ANN predictions showed 95% accuracy, outperforming regression models, supporting their use in automotive composites

Fibers were treated with 5–10 wt.% NaOH for up to 24 h to evaluate mechanical properties of single strands and multi-layer composites. A 5 wt.% NaOH of 24 h treatment yielded peak tensile strength of 159.16 MPa (single fiber), with the 5-layer composite showing 33.51 MPa tensile and 56.72 MPa flexural strength. This was found to be effective for automotive interior applications (Zalinawati *et al.* 2020). The kenaf/carbon/epoxy composite showed up to 1055% increase in flexural modulus and outperformed the glass counterpart, despite having a lower carbon fiber volume fraction. Significant improvements were recorded in all mechanical metrics over pure kenaf mat composites (Malik *et al.* 2022). Eco-composites were produced using four stacking configurations in resin. The Jute-Banana-Banana-Jute laminate showed the highest performance of 46.65 MPa tensile strength, 87.24 MPa flexural strength, and superior ILSS (30–43%) better than others. The SEM analysis revealed better fracture behavior due to jute on the outer surfaces (Prashanth *et al.* 2024). The influence of chemical treatment and fillers on fiber-epoxy composites was examined for mechanical, tribological, and water-resistant performance. Optimal results at 10% fly ash included 40.25 MPa tensile, 77.23 MPa flexural, and 44.82 kJ/m^2 impact strength. ANN showed reduced wear and moisture uptake, suitable for automotive and aerospace use (Sengottaiyan *et al.* 2025). Tri-layer composites were fabricated using palm leaf sheath and areca sheath fibers in varied stacking orders using the hand lay-up techniques. Composites with areca sheath skin and palm sheath core exhibited optimal 46 MPa tensile, 51 MPa flexural, and 54 MPa compressive strength. Reduced water absorption and good fiber-matrix adhesion were confirmed by SEM (Ganesh *et al.* 2020). Palm fibers were applied as a bio-adsorbent for removing violet methyl dye using solid-phase extraction and modeled by ANN. Parameters such as pH, contact time, rotation speed, and dosage were optimized. ANN modeling showed strong predictive power for dye removal performance, validated using RMSE, MAE, and correlation efficiency (Andayesh *et al.* 2020)

Research indicates that significant opportunities exist for further investigation of Banana-Palm amino resin composites. This study examined the option of palm and banana fibers within different directions in amino resin. An extensive statistical analysis utilizing machine learning methodologies such as ANN was used for predictive purposes. In the fabrication of composites, the woven eco-fiber laminate featuring inter ply orientations of 0/0/0/0/0/0 (S1), 0/45/0/0/45/0 (S2), 0/90/0/0/90/0 (S3), and +45/−45/+45/+45/−45/+45 (S4) were utilized. Additionally, tests and analyses were performed to evaluate the influence of palm and banana fiber orientations on surface morphology as well as mechanical properties, such as flexural strength, tensile strength, inter-laminar shear strengths, and impact energy.

2. MATERIALS AND METHODS

2.1 Materials

Banana and palm fiber mats were acquired from Go green enterprises, Chennai, India. The amino resin and TiO_2 nanoparticles were obtained from Matrix Enterprises, Nagercoil, Tamil Nadu, India. Table 1 illustrates the chemical and physical features of banana fiber and palm fiber and the characteristics of the amino resin are outlined in Table 2.

Table 1. Properties of banana fiber and palm fiber

Properties	Banana Fiber	Palm Fiber
Strain at break	1.0–3.5%	1–4%
Modulus	5–32 GPa	2–6 GPa
Tensile strength	355–770 MPa	190–370 MPa
Pectin	5%	5–10%
Cellulose	60–65%	35–50%
Lignin	5–10%	20–30%
Hemicellulose	15–20%	20–35%
Density	1.35–1.50 g/cm^3	1.20–1.45 g/cm^3

Table 2. Properties of amino resin

Properties	Amino Resin
Melamine content	White granular solid
Viscosity	30–60%
Appearance	50–65%
Solid content	50–500 mPa·s
Density	7.5–9.5
pH	1.25–1.35 g/cm^3

2.2 Fabrication of Banana-palm Amino Composite

The law of mixtures is employed to ascertain the optimal quantities of epoxy resin and fibers. Subsequently, composites were fabricated by applying a desired quantity of amino resin premixed with TiO_2 nanoparticles at 2, 4 6 and 8 wt.% concentration to palm and banana fibers. The TiO_2 nanoparticles were first ultrasonically dispersed in the amino resin for 30 minutes to ensure uniform distribution and minimize agglomeration. The resulting nanofilled resin was then used to impregnate the fibers. The composites were layered with designed fiber orientations. Composite fabrication method utilized in the study was taken from Balaji *et al.* (2024). Banana fiber particle and hybrid composites were fabricated by compression molding with epoxy as matrix. The subsequent step involved positioning the composites in a compression molding machine set to 120°C for 20 minutes at a pressure of 1 MPa. This method comprised of the concurrent application of temperature and pressure to produce a hybrid composite of TiO_2 reinforced with amino resin and Banana-Palm fibers. The composite samples were subsequently sectioned in compliance with ASTM requirements utilizing a wood cutting machine. Fig. 1 illustrates the various processes of manufacturing natural fiber composites. Table 3 depicts the different fiber orientation of the composites.

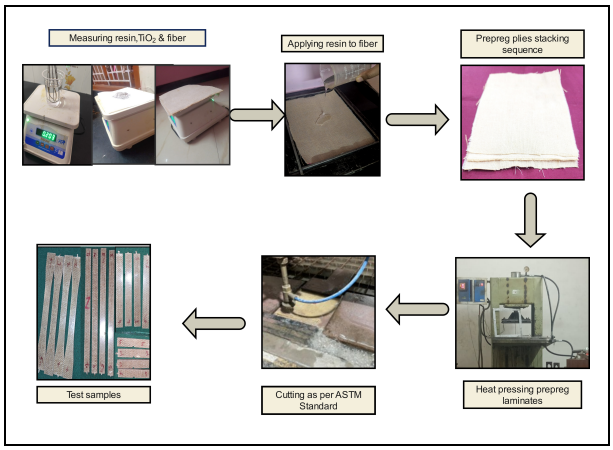
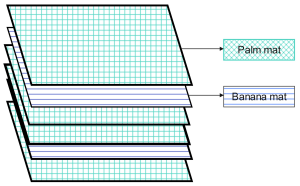


Fig. 1: Different stages of manufacturing hybrid banana-palm amino composites

Table 3. Different fiber orientations of the composites



Fiber alignment	0/0/0/0/0	0/45/0/0/45/0	0/90/0/0/90/0	+45/−45/+45/+45/−45/+45
Composite structure	S1	S2	S3	S4

2.3 Mechanical Properties of the Composite Specimens

Samples with dimensions of 25 mm width × 250 mm length × 3 mm thickness were used to test tensile strength using an Instron Universal Testing Machine (UTM) equipped with a 5 kN load cell at a crosshead speed of 2 mm/min, in compliance with ASTMD3039-14. Flexural properties were examined for a specimen with dimensions of 127 mm length, 12.7 mm width and 3 mm thickness. The test was performed according to the specifications established in ASTMD790-3, and the UTM equipped with 5 kN load cell capacity were used for the evaluation process. Composite samples were subjected to impact test utilizing 22 J hammer on a type XC-50 Pantec machine. The test specimen measured 12.7 mm in width, 64 mm in length, and 3 mm in thickness. The test procedure conformed to ASTMD256-10. The interlaminar shear strength were assessed utilizing a Z-RUTM with a load capacity of 5 kN, in accordance with ASTMD2344-00. The sample had a thickness of 3 mm, a breadth of 12 mm, and a length of 60 mm. Each batch contained five specimens that were tested. Their results were averaged and documented. The ZEISS FE-SEM, functioning at a voltage of 20 kV, was used to evaluate the surface morphology structures of fractured specimens. The primary objective of the investigation was to detect patterns of interfacial rupture in the tensile tests that were conducted.

2.4 Simulation of Artificial Neural Networks

Algorithms were run for making predictions to capture the essence of the connection between two sets of data, namely, input variables called predictors and output variables called responses. The model produces a transformation from the source variables to the output variables through an iterative learning process, with few or no assumptions regarding the prior model form. The predominant neural networks examined in connection with composites were multi-layered neural networks for tasks such as function estimation, pattern classification (Fig. 2), and pattern association. Multilayer feed-forward networks are capable of being trained using various transfer functions through backpropagation training. The input consisted of fiber orientation and reinforcement (wt%). The output data encompassed mechanical parameters such as TS (MPa), FS (MPa), and IS (J/m).

The sigmoid function, commonly known as the logistic function, is a transfer method often utilized in neural networks. Listed below are several grounds for its potential selection: The logistic function converts a real value within the range. This is beneficial for binary classification tasks aimed at generating a probability that reflects the likelihood of a specific class. Optimization methods, such as gradient descent, benefit from the sigmoid function's smooth and differentiable properties. During training, this property makes it easier to find the minimum of the loss function. For situations where a probability-like output is required, the sigmoid function is a good fit due its output and seen as a probability. Nonetheless, some restrictions and considerations exist: The vanishing gradient problem occurs because the logistic function compresses input parameters toward the limits of 0 or 1. The compression leads to the disappearance of gradients during backpropagation. This may impede the training process, particularly in deep learning models.

3. RESULTS AND DISCUSSION

3.1 Density and Void Content

The density values, both predicted then experimentally obtained for hybrid, banana palm amino resin composites are listed in Table 4, together within the attributed void content. Voids and other defects in the composite material cause the predicted and experimental densities to diverge.

Table. 4. Density and Void content for various hybrid eco-fiber composites

Composite	Fiber Orientation	Weight (grams)				Density(g/c.c.)		Void Content (%)
		Palm Fiber	Banana Fiber	Amino Resin	TiO_2	Theoretical	Experimental	
S1	0/0/0/0/0/0	60	60	120	2	1.21	1.19	1.65
S2	0/45/0/0/45/0,				4		1.18	2.47
S3	0/90/0/0/90/0,				6		1.19	1.65
S4	+45/−45/+45/+45/−45/+45				8		1.2	0.82

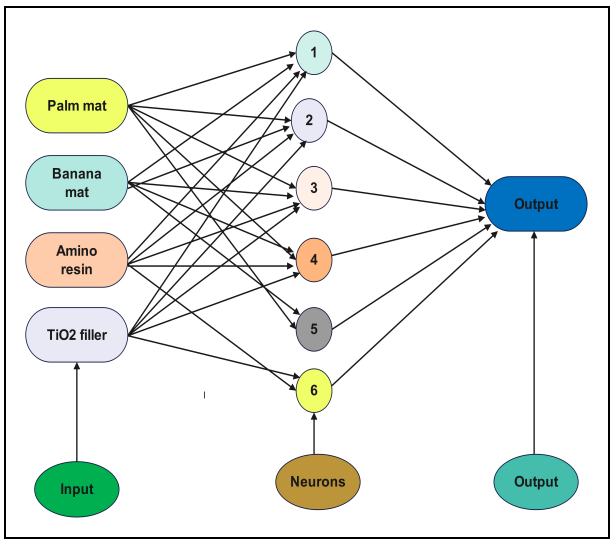


Fig. 2: ANN architecture for prediction of mechanical properties

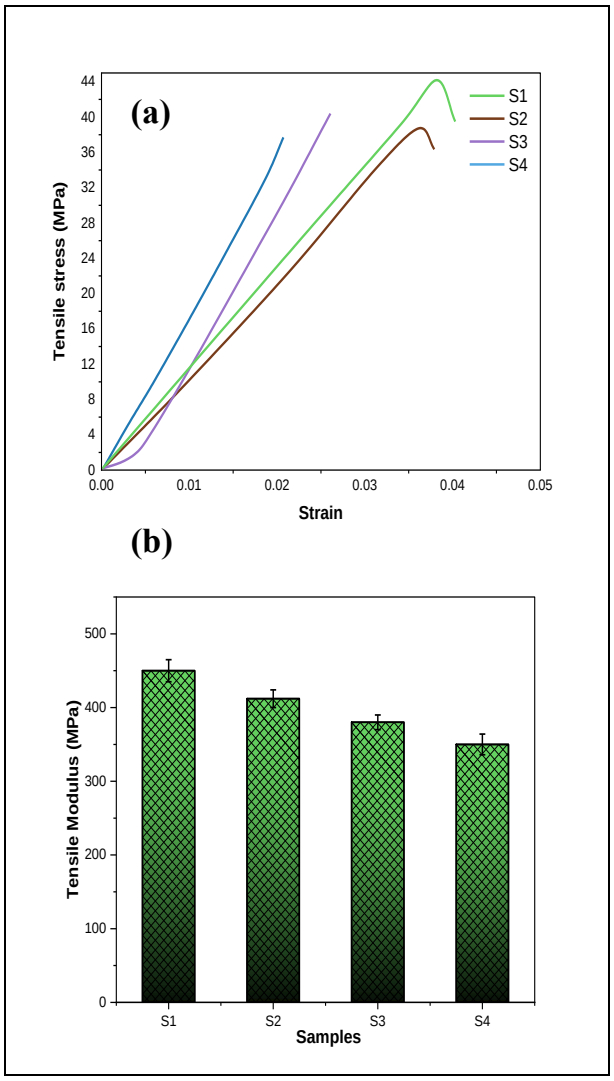


Fig. 3: (a) Tensile stress-to-strain graph (b) Tensile modulus for different hybrid composites

3.2 Results of Tensile Tests

As shown in Fig. 3(a), the deviation of the fibers from the direction of the applied load results in a reduction in composite strength, and all curves demonstrate low ductility. Composite S1 outperforms composites S2, S3, and S4 in terms of strength by 14%, 9%, and 16%, respectively. Fig. 3(b) shows that composite S1 has a tensile modulus that is 8%, 15%, and 22% higher when compared to composites S2, S3, and S4, respectively. Composite S1 has fibers that run perpendicular to the direction of the force. They are able to effectively withstand the stress because of how they pull together. Composites are not strong enough to endure tension since their fibers run perpendicular to the stress. The performance of the material depends increasingly on the modulus of the composite matrix, especially in S4 and S2, rather than the intrinsic strength of the fibers. The increase in fibers oriented at angles greater than 0° causes this shift because it puts more strain on the matrix and makes it more likely to fail. In this failure process, the characteristics and interactions of matrix material with the fibers are very important. In these conditions, the overall performance and durability of the composite structure are contingent upon the stress resistance of matrix and the interfacial bonding between the fibers and the matrix.

When analyzing unsaturated polyester resin composites reinforced by maintaining the alignment of fibers, an increasing number of fibers deviating from the load direction reduces performance. Composites with alternating layers tend to achieve high tensile strength (Gaddala *et al.* 2025).

3.3 Flexural Strength

Fig. 4(a) shows the load-displacement curve for different composites. The flexural modulus of composite S1 is 10%, 15%, and 23% superior to that of composites S2, S3, and S4, respectively (Fig. 4(b)). The FS of composite S1 is 8%, 16%, and 30% superior to that of composites S2, S3, and S4, respectively (Fig. 4(c)). In composite S1, fibers oriented at a 0° angle parallel to the applied load demonstrate uniform stress transmission and efficient weight distribution. This alignment enables enhanced load-bearing capability by uniformly distributing stress over the length of the fibers. Consequently, stress concentrations reduce, thereby enhancing flexural strength and resistance to failure. Nevertheless, the fibers in composites S2 and S4 are not oriented along the direction of the applied tension, leading to reduced efficiency in load transfer. The regions where the fibers terminate or where gaps exist frequently endure increased stress upon the application of a load. Fractures may form more readily in composite S3 because the perpendicular orientation of the fibers to the load, thus, reducing their resistance to the applied stress throughout their length. Boban *et al.* (2025) have also

reported that hybrid composites reinforced with banana fiber display high flexural strength.

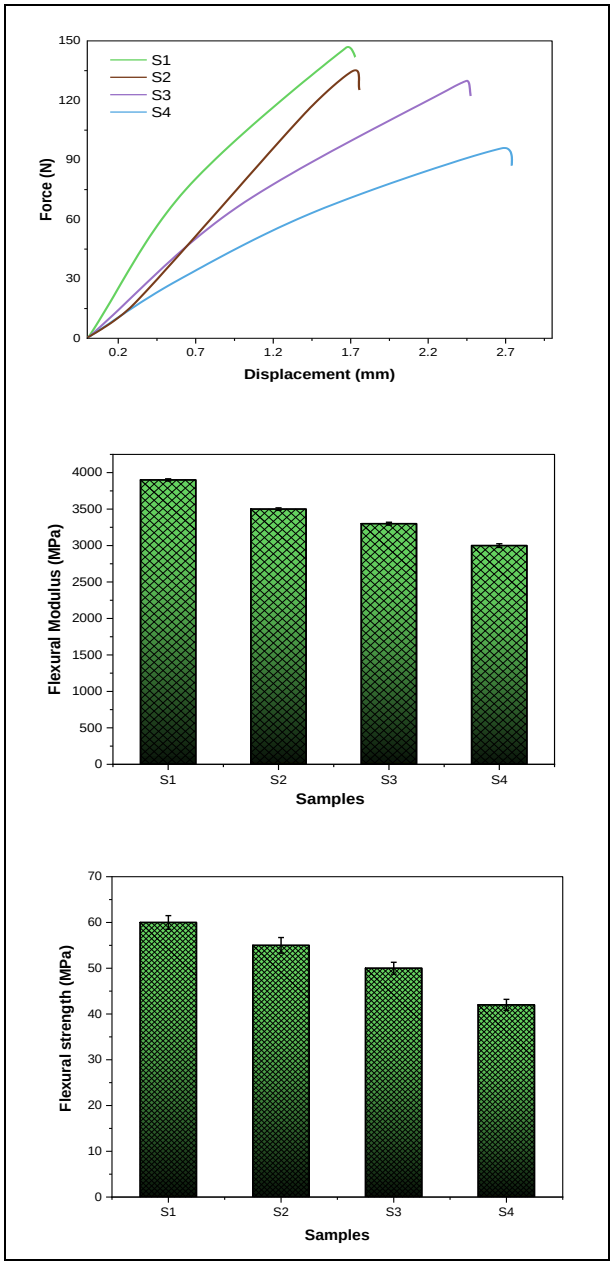


Fig. 4: Comparative plots showing (a) force displacement characteristics, (b) flexural modulus and (c) FS of diverse banana-palm hybrid amino matrix materials

3.4 Impact Strength

Composites S1 (Fig. 5) exhibited superior impact strength, surpassing composites S2, S3, and S4 by 9%, 13%, and 16%, respectively. The orientation of fibers significantly influences the impact resistance of composites. The fibers of banana-palm composites aligned perpendicularly to the trajectory of the impact force may yield specific effects. The orientation of the fibers perpendicular to the impact force increases their ability to resist force and distribute stress over a broader region. This configuration allows the fibers to act as barriers, they absorb and dissipate impact energy, thereby improving impact resistance.

In comparison to other directions, the right-angled fibers exhibit superior impact properties due to their enhanced ability to endure force. The impact strength of S2 and S3 composites has reduced due to fiber deviation from 0°. conversely, the impact strength of S4 composite was the lowest, resulting from the absence of fiber alignment perpendicular to the applied impact force. Hybrid composites were fabricated with alkali-treated fibers. Type I showed highest impact energy, while Type III exhibited the best dynamic and mechanical properties including a higher break load as reported by (Murali *et al.* 2023).

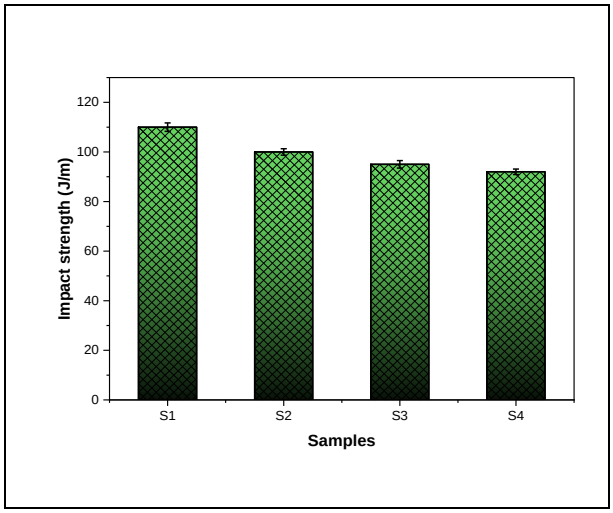


Fig. 5: Comparison of the impact strength of different hybrid banana palm amino resin composites

3.5 Interlaminar Shear Strength Assessment

Fig. 6(a) presents the force–displacement relationship, which demonstrates the material characteristic load-bearing behavior. Composites S1 possesses superior load-bearing capability attributable to enhanced matrix bonding compared to the other composites. Fig. 6(b) presents the ILSS values of composites. Composite S1 exhibits superior strength values (33%, 18%, and 30%) relative to composites S2, S3, and S4. Fiber laminates with this stacking configuration exhibited higher ILSS as also observed by Xiao *et al.* (2024). The maximal ILSS is typically observed in composite S1, where the fibers were oriented along the 0° direction parallel to the applied load and demonstrated enhanced strength. This orientation enhances the capacity of the fibers to endure load while countering shear stresses. As the angle of fiber alignment moves away from 0°, however, the ILSS drops. Discordance between the direction of the applied force and the fiber reinforcement caused by different

orientations reduces resistance of the composites to shear stresses. The degree of reduction is determined by the fiber angle. As a result, the interlaminar shear strength is typically lower at 45° than at 0°, and it drops off sharply as the fiber angle increases.

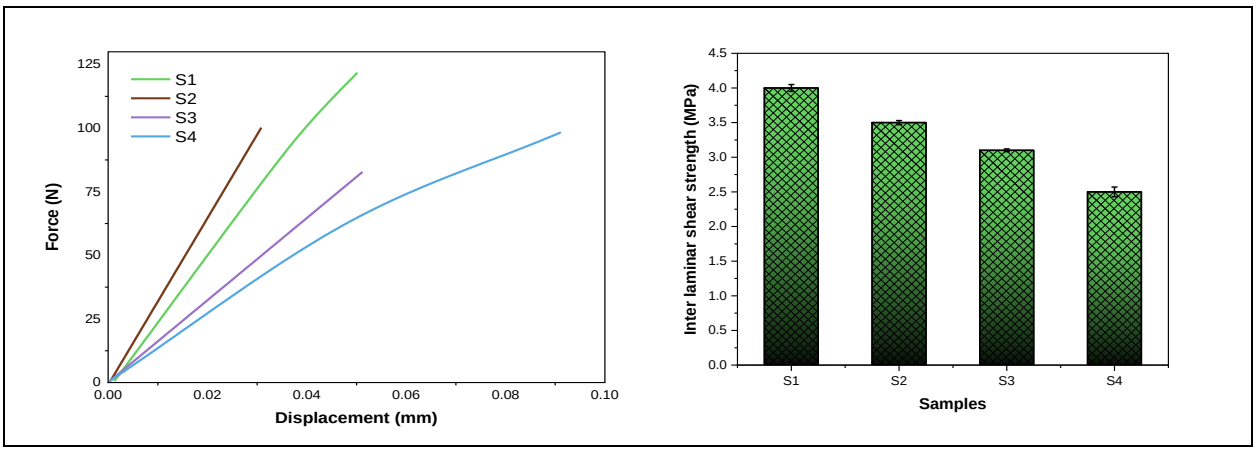


Fig. 6: (a) Load Vs displacement curve and (b) ILSS of different hybrid composites

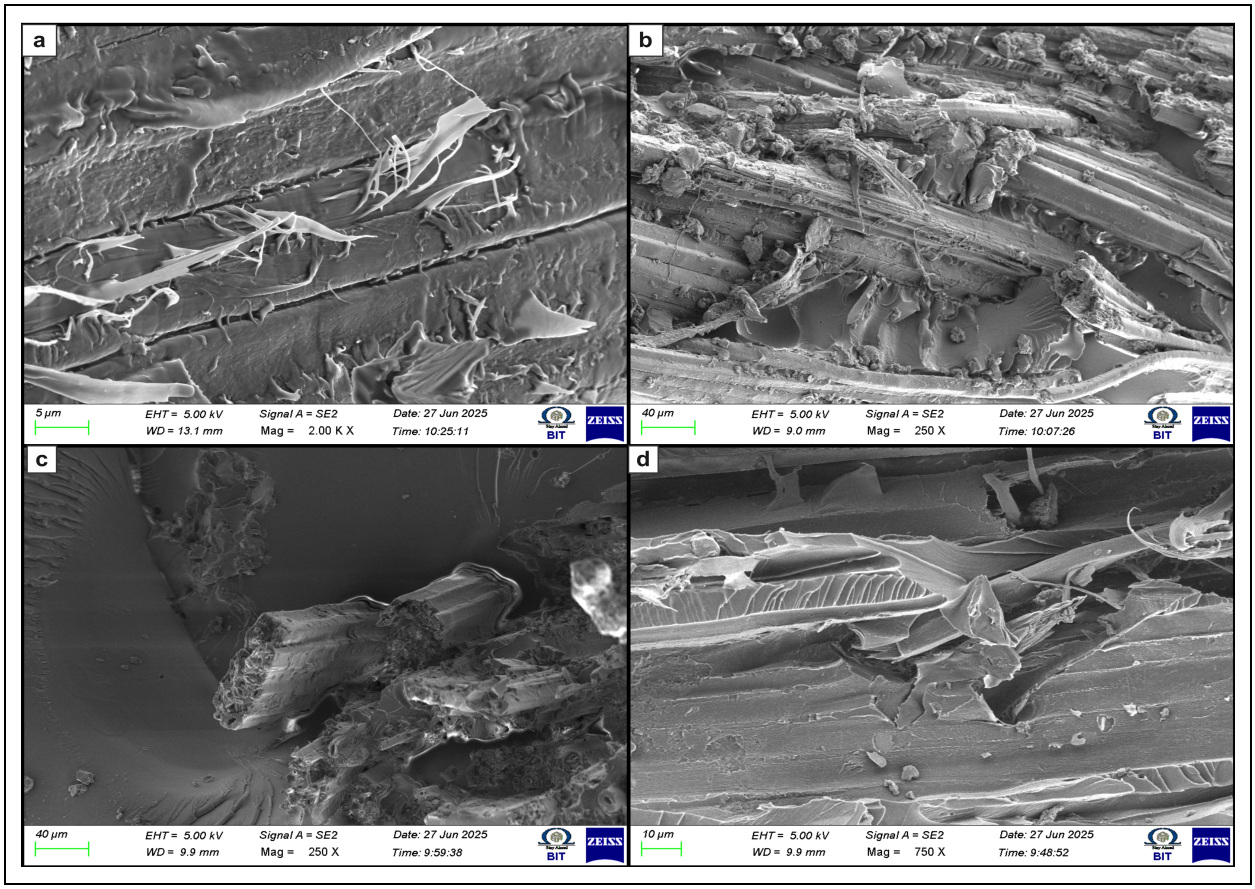


Fig. 7: SEM images of fractured surface of the tensile-tested composites for various fiber orientations (a) S1 (b) S2 (c) S3 and (d) S4 composites

3.6 Surface Morphology Analysis

Fig. 7 (a–d) present the SEM images of the fractured surfaces of natural fiber-reinforced polymer composites, elucidating essential aspects of fiber-matrix interface adhesion and failure mechanisms following mechanical loading. Fig. 7(a) illustrates the surface morphology of composite S1, demonstrating robust interfacial adhesion between the fiber and matrix. The SEM images confirmed superior fiber–matrix bonding as observed by Shivayogi *et al.* (2024). The low fiber pull-out and distinct fiber impressions indicate efficient load

transfer and mechanical interlocking. The cohesive failure mechanism, together with the dense structure and minimal void content, verifies effective dispersion and wetting of the fibers inside the matrix, hence enhancing mechanical characteristics. Fig. 7(b) pertains to composite S2, exhibiting more prominent indications of interfacial debonding. The observable fiber pull-outs and surface irregularities indicate diminished fiber-matrix adhesion. Cracks advancing at the fiber-matrix interface indicate diminished capacity to impede crack propagation, resulting in premature failure under tensile stress. Fig. 7(c) illustrates the microstructure of composite S3, marked by evident indications of matrix fracture and fiber rupture. The fractured fiber termini and matrix disintegration signify a brittle failure mechanism. Inadequate interfacial contact is seen, possibly leading to inefficient stress transfer and diminished tensile strength. Fig. 7(d) illustrates composite S4, characterized by matrix cracking, fiber pull-out, and surface delamination. The comparatively clean fracture surface, coupled with the presence of voids and fiber separation, indicates inadequate bonding. These qualities collectively emphasize the imperative for enhanced fiber treatment or matrix alteration to increase composite performance. The SEM images highlight the essential significance of fiber-matrix interaction, fiber dispersion, and structural compatibility in determining the mechanical properties of natural fiber-reinforced composites.

3.7 ANN Projected Results

Fig. 8 illustrates the correlation between the output of the network and the projected targets through regression curves. As part of the network verification process, regression curves were constructed to evaluate the degree of agreement between the target data and the network's predictions. The correlation coefficients for each regression curve were 0.9578, 0.9872, and 0.9542. Values approaching 1 indicate that the model exhibits a strong fit, with excellent predictive accuracy and correlation. As shown by the regression curves, the data points closely follow the ideal line of fit, indicating a strong correlation and a high level of agreement between the network's output and the expected targets. High R-values nearing 1 in the regression curves for training and validation confirm the model's strong predictive accuracy and correlation with target outputs. The dataset comprised 120 entries, with 84 used for model training and the remaining 36 reserved for testing and validation purposes. Fig. 8 shows a clustering of the majority of data points, implying that only a subset of the full dataset is visually displayed. The observed results indicate that performance enhancement is achieved by progressively refining the network's connections through repeated modifications of weights and biases. Similarly, in a study by Saravanakumar *et al.* (2024), the results were accurately predicted by ANN, achieving R^2 values above 0.95.

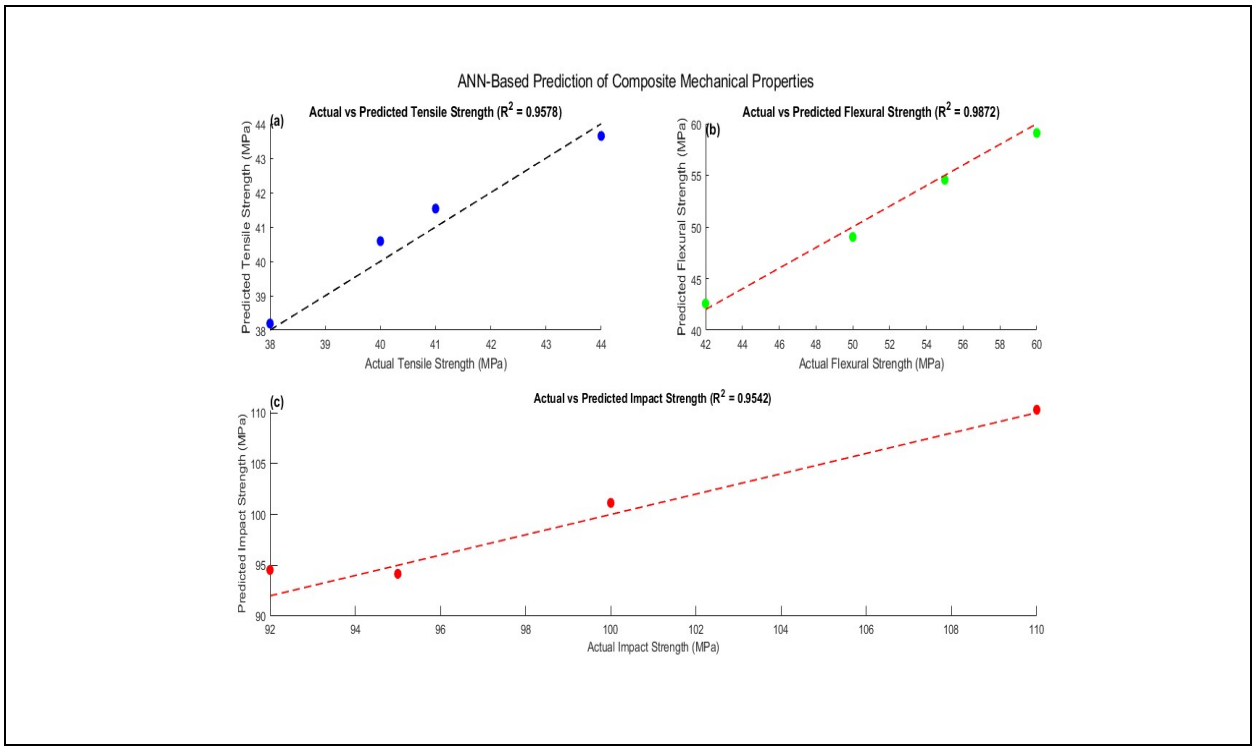


Fig. 8: Comparison of predicted and actual values for (a) tensile strength, (b) flexural strength and (c) impact strength

4. CONCLUSION

The experimental results confirmed that fiber orientation strongly influenced the mechanical performance of banana–palm amino composites reinforced with TiO_2. Composite S1, fabricated with fibers aligned at 0°, achieved the best results, recording a tensile strength of about 68 MPa, tensile modulus of 3.25 GPa, flexural strength of 72 MPa, flexural modulus of 3.9 GPa, interlaminar shear strength of 4 MPa, and impact strength of 110 J/m. In comparison, Composite S3 showed lower performance, with tensile and flexural strengths of 62 MPa and 60 MPa, respectively, interlaminar shear strength of 3.2 MPa, and impact strength of 95 J/m, while Composite S4 exhibited further reductions, with tensile strength of 58 MPa, flexural strength of 55 MPa, interlaminar shear strength of 2.8 MPa, and impact strength of 90 J/m. Composite S2, despite showing the highest density of 1.18 g/cm³ and void content of 2.47%, displayed weaker properties across all tests due to increased porosity. SEM analysis revealed strong fiber–matrix adhesion in S1 and poor bonding in S2–S4, confirming that microstructural integrity is closely tied to mechanical behavior. ANN predictions further supported these findings, with high correlation values (R^2 = 0.9578 for tensile strength, 0.9872 for flexural strength, and 0.9542 for impact strength), demonstrating excellent agreement between experimental and predicted data. These results establish S1 as the most effective fiber orientation for achieving superior mechanical performance in banana–palm amino composites

FUNDING

This research received no specific grant from any funding agency in the public, commercial, or not-for-profit sectors.

CONFLICTS OF INTEREST

The authors declare that there is no conflict of interest.

COPYRIGHT

This article is an open-access article distributed under the terms and conditions of the Creative Commons Attribution (CC BY) license (http://creativecommons.org/licenses/by/4.0/)

REFERENCES

Andayesh, R., Abrishamkar, M. and Hodaee, H., Using Artificial Neural Network Modeling in Predicting the Amount of Methyl Violet Dye Absorption by Modified Palm Fiber, *J. Sci., Islamic Republic Iran.,* 31(3), 221–231(2020). https://doi.org/10.22059/jsciences.2020.286177.1007433

Arunachalam, S. J. and Saravanan, R., Comprehensive Insights of Chemically Treated Jute/Kenaf/Glass Fiber with TiO_2 Nanoparticle using RSM Optimization, *J. Environ. Nanotechnol.,* 13(2), 21–30(2024). https://doi.org/10.13074/jent.2024.06.242564

Balaji, A., Kannan, S., Purushothaman, R., Mohanakannan, S., Maideen, A. H., Swaminathan, J., Karthikeyan, B. amd Premkumar, P., Banana fiber and particle-reinforced epoxy biocomposites: mechanical, water absorption, and thermal properties investigation, *Biomass Convers. Biorefin.,* 14(6), 7835–7845(2024). https://doi.org/10.1007/s13399-022-02829-y

Balan, P., Priyadharshini, G. S., Divakaran, D., Suyambulingam, I., Sunesh, N. P., Rangappa, S. M. and Siengchin, S., Microcrystalline cellulose extraction from comprehensive characterization of Mangifera indica leaf biowaste for high-performance bio-based polymer composites, *J. Polym. Res.,* 32(1), 23(2025). https://doi.org/10.1007/s10965-024-04251-6

Banu, M., Madhavan, V. R. B., Manickam, D. and Devarajan, C., Experimental investigation on stacking sequence of Kevlar and natural fibres/epoxy polymer composites, *Polim.,* 31(1), e2021004 (2021). https://doi.org/10.1590/0104-1428.04320

Benyettou, R., Amroune, S., Mohamed, S., Seki, Y. and Dufresne, A., Experimental Investigation of the Absorption Behavior of Date Palm Fiber Reinforced Iso-Polyester Composites: Artificial Neuron Network (ANN) Modeling, *J. Nat. Fibers.,* 19(17), 15902–15918(2022). https://doi.org/10.1080/15440478.2022.2136323

Boban, A. P., Mishra, D. K., Kumar, N., Kumar, S., Mahakur, V. K. and Sharma, S., Quasi-static indentation, mechanical, and damage evolution of different configurations of laminated banana–pineapple fiber-reinforced composites for structural application, *Text. Res. J.,* xxxx, xx(2025). https://doi.org/10.1177/00405175251322952

Gaddala, B., Kandavalli, S. R., Raghavendran, G., Sivaprakash, A., Rallabandi, R., Sundramurthy, V. P., Selvaraju, M. and Sugumar, M., Exploring the impact of hybridization on green composites: Pineapple leaf and sisal fiber reinforcement using poly(furfuryl alcohol) bioresin, *Z. Phys. Chem.,* 239(4), 495–518(2025). https://doi.org/10.1515/zpch-2024-0772

Ganesh, S., Gunda, Y., Mohan, S. R. J., Raghunathan, V. and Dhilip, J. D. J., Influence of Stacking Sequence on the Mechanical and Water Absorption Characteristics of Areca Sheath-palm Leaf Sheath Fibers Reinforced Epoxy Composites, *J. Nat. Fibers.,* 1–11(2020). https://doi.org/10.1080/15440478.2020.1787921

Giridharan, M. R. and Sivaganesan, S., optimization of interlaminar shear strength of kevlar/waste-based piassava fiber nano-sio2 hybrid composites by response surface methodology, *J. Balkan Tribological Assoc.,* 31(2), 249–264 (2025).

Girimurugan, R., Sahoo, G., Sivalingam, A. and Mayakannan, S., Effect of nano alumina powder and water hyacinth stem powder addition on tensile properties of polypropylene matrix hybrid composites – An experimental study, *Mater. Today Proc.,* 60, 2099–2104(2022). https://doi.org/10.1016/j.matpr.2022.01.477

Gowrishankar, R., Sithar, S. P. M., Narayana, K. S., Raja, T., Gokul, R. and Mayakannan, S., Design and Optimization of a Biocompatible Polyethylene Composite with Nelumbo Nucifera Fiber and Nano-banana Peel Filler for Sustainable Environmental Applications, *J. Environ. Nanotechnol.,* 14(1), 306–322(2025). https://doi.org/10.13074/jent.2025.03.2441019

Kandavalli, S. R., Sundramurthy, V. P., Krishnasamy, V. D., Prasad, G. N. R., Kasi, U. K., Rajesh, S., Kumar, B. R., Selvaraju, M., Kadaikunnan, S. and Khaled, J. M., Bioresin based hybrid green composite preparation using Holoptelea integrifolia fibers reinforced by Ziziphus jujuba seed particles: a fuzzy logic assisted optimization of mechanical behaviour, *Z. P. Chem.,* 239(5), 747–772(2025). https://doi.org/10.1515/zpch-2024-0837

Krishnasamy, B., Thirugapillai, P., Rajakannu, A. and Selvaraju, M., Optimization and multi-objective analysis of tensile, flexural and impact strength in nano-hybrid bio-composites reinforced with Helicteres isora, Holoptelea integrifolia fibers, and nanographene, *Rev. Materia.,* 30(1), e20240864(2025). https://doi.org/10.1590/1517-7076-RMAT-2024-0864

Kumar, S. S., Shyamala, P., Pati, P. R., Giri, J., Makki, E. and Sathish, T., Mechanical (static and dynamic) characterization and thermal stability of hybrid green composites for engineering applications, *J. Mater. Res. Technol.,* 30, 7214–7227(2024). https://doi.org/10.1016/j.jmrt.2024.05.132

Makri, H., Amroune, S., Zaoui, M., Saada, K., Jawaid, M., Seki, Y., Aichouche, B., Fouad, H. and Uddin, I., Investigation on the Mechanical Behavior of Date Palm Fibers Reinforced Composites: Predictive Modelling Using Artificial Neural Networks (ANNs), *J. Nat. Fibers.,* 21(1), 2396899(2024). https://doi.org/10.1080/15440478.2024.2396899

Malik, K., Ahmad, F., Yunus, N. A., Gunister, E., Dawood, M. S. I. S., Ali, S., Mani, C. S., Syahir, M. and Larry, A. L., The Hybridization Effects of Glass and Carbon Fibers on the Mechanical Properties of Kenaf Mat/Epoxy Composites, *J. Nat. Fibers.,* 19(17), 15432–15447(2022). https://doi.org/10.1080/15440478.2022.2127437

Murali, B., Karthik, K., Marotrao, S. S., Laxmaiah, G., Yadav, A. S., Prasanth, I. S. N. V. R. and Abbas, M., Mechanical and dynamic mechanical properties of hybrid kevlar/ natural fiber composites, *Mater. Res. Express.,* 10(10), 105305(2023). https://doi.org/10.1088/2053-1591/ad02e1

Muralidharan, M., Sathishkumar, T. P., Rajini, N., Navaneethakrishan, P., Ismail, S. O., Senthilkumar, K., Siengchin, S., Mohammad, F. and Al-Lohedan, H. A., Ply-stacking effects on mechanical properties of Kevlar-29/banana woven mats reinforced epoxy hybrid composites, *J. Ind. Text.,* 52. 1528083722118024(2022). https://doi.org/10.1177/15280837221128024

Natrayan, L., Surakasi, R., Patil, P. P., Kaliappan, S., Selvam, V. and Murugan, P., Optimizing Numerous Influencing Parameters of Nano-SiO2/Banana Fiber-Reinforced Hybrid Composites using Taguchi and ANN Approach, *J. Nanomater.,* 2023(1), 3317584(2023). https://doi.org/10.1155/2023/3317584

Prashanth, B. H. M., Ramesh, S., Gouda, P. S. S., Naik, G. M., Sharma, P., Jagadeesh, C., Math, M. M. and Anne, G., Impact of ply stacking sequence on the mechanical response of hybrid Jute-Banana fiber phenoplast composites, *Mater. Res. Express.,* 11(5), 055301(2024). https://doi.org/10.1088/2053-1591/ad425c

Saravanakumar, S., Sathiyamurthy, S., Pathmanaban, P. and Devi, P., Integrating machine learning and response surface methodology for analyzing anisotropic mechanical properties of biocomposites, *Compos. Int.,* 31(1), 1–28(2024). https://doi.org/10.1080/09276440.2023.2260239

Sengottaiyan, S., Sathiyamurthy, S., Selvakumar, G. and Haridass, R., Influence of treatment and fly ash fillers on the mechanical and tribological properties of banana fiber epoxy composites: experimental and ANN-RSM modeling, *Compos. Int.,* 32(7), 953-985(2025). https://doi.org/10.1080/09276440.2024.2448879

Shivayogi, B. H., Manjunatha, T. S., Gouda, P. S. S., Prashanth, B. H. M. and Pai, M. P., Influence of layering sequence on performance of jute/wool epoxy hybrid composites: a comparative study with automotive plastic, *Eng. Res. Express.,* 6(1), 015522(2024). https://doi.org/10.1088/2631-8695/ad2ef8

Shubham, S. K., Pandey, A. and Purohit, R., Development and Investigation of Biodegradable Hybrid Fiber Sandwiched Composites Using Ultrasonication, *Polym. Adv. Technol.,* 35(12), e70042(2024). https://doi.org/10.1002/pat.70042

Singh, G., Gairola, S., Singh, I. and Sham, S. R., Mechanical, thermal, and flammability behavior of chitosan-modified date palm leaf–based polypropylene composites, *Biomass Convers. Biorefin.,*(2024). https://doi.org/10.1007/s13399-024-06085-0

Tang, X., Liu, Q., Bai, Z., Li, L. and Hu, Y., Effect of stacking order on the properties of hybrid palm sheath/polyester fiber felt-reinforced polymer composite laminates, *Polym. Compos.,* 45(7), 6525–6535(2024). https://doi.org/10.1002/pc.28215

Venkatesh, R., Alkali Process Coir Natural Fiber Incorporated Epoxy Composite Made by Compression Mold Route: Characteristics Evaluation, *J. Inst. Eng. India Ser. D.,* (2024). https://doi.org/10.1007/s40033-024-00723-7

Vijayakumar, A. A., Prasad, V. and Kochunny, M. K., Investigation on the effect of stacking order and hybridization on mechanical and water absorption properties of woven flax/bamboo composite, *Polym. Compos.,* 43(8), 5189–5207(2022). https://doi.org/10.1002/pc.26808

Xiao, H., Sultan, M. T. H., Shahar, F. S. and Nayak, S. Y., Mechanical and Viscoelastic Behavior Characterization of Hybrid Aluminum/Carbon Fiber/Pineapple Leaf Fiber Composite via VARTM for Automotive Industry, *J. Nat. Fibers.,* 21(1), 2382874(2024). https://doi.org/10.1080/15440478.2024.2382874

Yuhari, S. F. and Awang, A., Effect of oil palm fiber on mechanical properties of sandwich-structured glass, *Sci. Eng. Health Stud.,* 17, 23020002(2023). https://doi.org/10.14456/sehs.2023.2

Zalinawati, M., Siregar, J. P., Tezara, C., Jaafar, J., Hamdan, M. H. M., Oumer, A. N. and Rihayat, T., Effect of Surface Modification on Mechanical Properties of Buri Palm (Corypha Utan) Fibre Composite Reinforcement, *Int. J. Autom. Mech. Eng.,* 17(4), 8298–8309(2020). https://doi.org/10.15282/ijame.17.4.2020.07.0627